Laser Physics Letters

Astro Ltd.

LETTER

Low-intensity-noise single-frequency CW 1080 nm laser by employing a laser crystal with the small stimulated-emission cross section

To cite this article: Huiqi Yang *et al* 2022 *Laser Phys. Lett.* **19** 055801

View the article online for updates and enhancements.

You may also like

- $AuGa_2$ on focused Ga ion beam-fabricated Au nanorod array for trace detection of melamine cyanurate in milk solution
Kundan Sivashanmugan, Jiunn-Der Liao, Bernard Haochih Liu et al.
- Room temperature diode-pumped $Yb:CaYAlO_4$ laser with near quantum limit slope efficiency
W D Tan, D Y Tang, X D Xu et al.
- A stable gain-switched Ho:CYA laser resonantly pumped at 1922 nm
J N Zhang, B H Chen, D Y Shen et al.



IOP ebooks™

Bringing together innovative digital publishing with leading authors from the global scientific community.

Start exploring the collection–download the first chapter of every title for free.

This content was downloaded from IP address 115.24.1.4 on 21/03/2022 at 11:45

IOP Publishing | Astro Ltd Laser Physics Letters
Laser Phys. Lett. **19** (2022) 055801 (7pp) https://doi.org/10.1088/1612-202X/ac5b5d

Letter

Low-intensity-noise single-frequency CW 1080 nm laser by employing a laser crystal with the small stimulated-emission cross section

Huiqi Yang[1], Hailong Wang[1], Jiaqi Song[1], Pixian Jin[1,2], Xiaodong Xu[3], Jun Xu[4] and Huadong Lu[1,2,*]

[1] State Key Laboratory of Quantum Optics and Quantum Optics Devices, Institute of Opto-Electronics, Shanxi University, Taiyuan 030006, People's Republic of China
[2] Collaborative Innovation Center of extreme Optics, Shanxi University, Taiyuan 030006, People's Republic of China
[3] Jiangsu Key Laboratory of Advanced Laser Materials and Devices, School of Physics and Electronic Engineering, Jiangsu Normal University, Xuzhou 221116, People's Republic of China
[4] School of Physics Science and Engineering, Institute for Advanced Study, Tongji University, Shanghai 200092, People's Republic of China

E-mail: luhuadong@sxu.edu.cn

Received 14 February 2022
Accepted for publication 2 March 2022
Published 21 March 2022



Abstract

An effective approach to obtain a single-frequency laser with low intensity noise is presented in this paper, which is implemented by employing a gain medium with the small stimulated-emission cross section (SECS). When the adopted Nd:YAP ($Nd:YAlO_3$) gain medium with SECS of 4.6×10^{-19} cm^2 is replaced by Nd:CYA ($Nd:CaYAlO_4$) gain medium with SECS of 1.04×10^{-19} cm^2, the frequency of measured intensity noise reached shot noise limit obviously reduces from 2.49 to 1.5 MHz, which agrees well with the theoretical predictions. On this basis, a single-frequency continuous-wave (CW) Nd:CYA laser with low intensity noise is first achieved. The attained output power of the Nd:CYA laser is 1.12 W. The achieved single-frequency CW 1080 nm laser will satisfy the requirements of the squeezed and entangled light generation.

Keywords: 1080 nm laser, $Nd:CaYAlO_4$ crystal, low intensity noise, stimulated-emission cross section

(Some figures may appear in color only in the online journal)

1. Introduction

Solid-state single-frequency continuous-wave (CW) lasers have attracted considerable attentions because of their excellent characteristics including low intensity noise, perfect beam quality as well as high stability. And they have been applied to many fields ranging from cold atom physics [1, 2], quantum information [3] to gravitation wave detection [4]. Especially, in the generation of the continuous variable two-mode squeezed state light field via optical parametric oscillator (OPO) or optical parametric amplifier (OPA) with only

* Author to whom any correspondence should be addressed.

 © 2022 Astro Ltd

one potassium titanyl phosphate (KTP) crystal [5, 6], single-frequency dual-wavelength CW 1080/540 nm laser is the optimal candidate since the 1080 nm laser can just satisfy the α-cut type-II non-critical phase-matching condition of KTP crystal. Based on this phase-matching condition, the fundamental-wave 1080 nm laser and second-harmonic-wave 540 nm laser act as signal and pump fields, respectively, and then the two-mode squeezed state light field with perpendicular polarization direction can be easily generated. At the same time, it is also known that the squeezing degree of the squeezed state light is inversely proportional to the detection frequency of the generated squeezed state [5–7], which means that the lower the detection frequency is, the higher the squeezed degree of the achieved squeezed state light is. However, due to the contributions of several noise sources including pump source fluctuation, spontaneous-emission noise, dipole fluctuation noise, vacuum noise coupled from the output coupler and the noise introduced by the intracavity loss, the intensity noise of the traditional single-frequency CW laser at the frequency range of several MHz is so high that the squeezed degree of the achieved squeezed state light is seriously restricted. In order to further increase the squeezed degree of the two-mode squeezed state to realize quantum key distribution, entanglement swapping, deterministic quantum teleportation of coherent states, and so on, it is necessary to achieve a low-intensity-noise 1080 nm laser.

So far, several representative methods to suppress the intensity noise of lasers have been developed. In 1997, Lam *et al* successfully suppressed the intensity noise of the laser by using an electro-optic feedback technology [8]. Similarly, Zhang *et al* suppressed the laser intensity noise at the low frequency range and resonant relaxation oscillation (RRO) peak by feed-forward controlling the drive current of the pump laser diode in 2003 [9]. In 2011, Winkelmann *et al* achieved the goal of intensity noise suppression by locking the frequency of the slave oscillator to master laser with low intensity noise [10]. Willkie *et al* and Chen *et al* separately employed Fabry–Perot ring cavity as the mode cleaner to significantly filter high frequency noise of Nd:YAG laser [11] and Nd:YVO_4 laser [12] successfully in 1998 and 2001. Recently, Yu *et al* made further efforts to reduce the intensity noise of Nd:$YAlO_3$ (Nd:YAP) laser from 1.5 MHz to 300 kHz and improve the frequency stabilization by employing an ultra-low expansion high-finesse Fabry–Perot cavity as a frequency reference combined with cascade Pound-Drever-Hall laser stabilization system [13]. Although the methods mentioned above could usually be employed in the experiment to suppress the intensity noise of single-frequency lasers, the achieved laser systems are inevitable to be complex and susceptible to external devices. Another method to suppress the intensity noise of the single-frequency laser is manipulating the parameters of the single-frequency laser itself. With the development of lasers, traditional laser technologies can't satisfy the requirements of novel lasers. Especially, when the intensity noise is considered in the process of the laser design, the parameters of lasers including the gain medium and the resonator must be re-optimized. In 2018, our group effectively suppressed the intensity noise of the single-frequency laser by lengthening the laser resonator length to 1 m [7]. As a result, the mode-cleaner had been successfully fired and the intensity noise of the laser could reach the shot noise limit (SNL) at 1 MHz. Recently, we have further compared the influence of the pump scheme on the intensity noise of the laser and concluded that the traditional pump scheme was easier to attain a low-intensity-noise output because the traditional pump scheme could effectively reduce the dipole coupling between the active atoms and the laser cavity [14]. Different from the previous methods, in this paper, we propose a new approach to suppress the intensity noise of the laser, which is implemented by employing a gain medium with the small stimulated-emission cross section (SECS). Based on the proposed approach, a stable single-frequency 1080 nm laser with low-intensity-noise operation is successfully attained.

According to the intensity-noise spectrum theory, the transfer-function formula affected by various noise sources could be expressed as [7, 12, 15, 16],

$$V_f = k_1(\omega_r,\gamma_l)V_{vac} + k_2(\omega_r,\gamma_l)V_p + k_3(\omega_r,\gamma_l)V_{spont} + k_4(\omega_r,\gamma_l)V_{dipole} + k_5(\omega_r,\gamma_l)V_{losses}, \quad (1)$$

where V_{vac} indicates the vacuum noise caused by the output coupler, V_p, V_{spont}, V_{dipole} and V_{losses} represent the noises input from pump-source, spontaneous-emission, dipole fluctuation and intracavity losses, respectively. When the intensity noise spectrum of the laser normalized to the SNL, $V_{vac} = V_{spont} = V_{dipole} = V_{losses} = 1$, and V_p represents the actual intensity of the pump field. k_1, k_2, k_3, k_4 and k_5 are the corresponding functions of ω_r and γ_l. ω_r, expressed as $\omega_r = \sqrt{2\kappa G\alpha^2}$, is the frequency of the RRO. γ_l is the frequency of the damping rate of the RRO and expressed as $\gamma_l = G\alpha^2 + \Gamma + \gamma_t$. κ is the total photon decay rate, which is induced by output coupler loss and intracavity loss. α^2 is the intracavity photon number per atom of the lasing mode, Γ and γ_t are the pump rate and the atomic spontaneous emission rate from upper level to lower level, respectively. Other noise components coupled from mechanical and thermal noises usually dominate the low-frequency region far below 200 kHz [17–19], the corresponding noises would not be described in detail here. According to equation (1), for a given resonator and pump rate of the laser, ω_r, γ_l and the cutoff frequency of intensity noise only depend on the parameter of the stimulated emission rate (SER) G, and G is expressed as,

$$G = \frac{\sigma_s \rho c l}{nL}, \quad (2)$$

where σ_s is the SECS, ρ and n represent the atomic density and refractive index of crystal respectively, l and L are the lengths of gain medium and total laser cavity respectively, c is the light speed. From equation (2), G is only decided by the SECS of gain medium when other parameters are ensured. In other words, when rare earth ions are doped in a series of crystal hosts, the smaller the SECS of gain medium, the weaker the coupling dynamics between the population inversion and

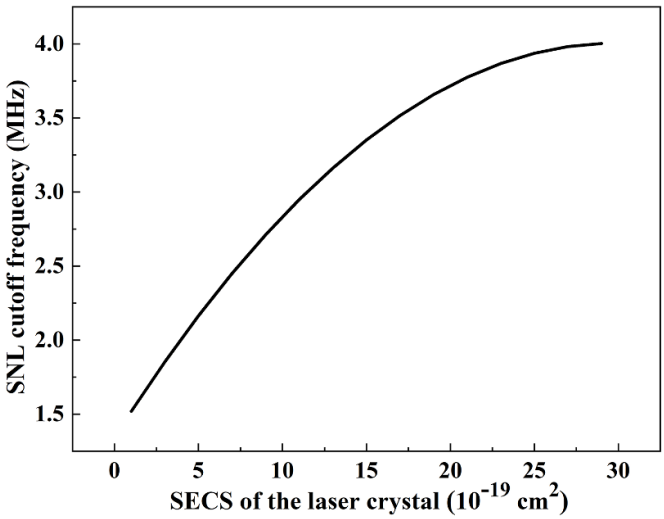


Figure 1. Theoretical prediction of the SNL cutoff frequency versus the SECS of the laser crystal.

Table 1. Simulation parameters.

Parameters	λ_{pump} (nm)	V_p (dB)	ρ (at. %)	n	l (mm)	L (mm)	P_{pump} (W)
Value	808	43.04	1	1.92	6	283.84	13.78

intracavity photons, which results in lower coupling strength of all noise sources in the laser field. In figure 1, the dependence of SNL cutoff frequency versus SECS of laser crystal is simulated under the same conditions of resonator and gain medium, except the SECS of laser crystal. The detailed simulation parameters are presented in table 1, where λ_{pump} and P_{pump} indicate the wavelength and input power of the pump source, respectively. It is obvious that the SNL cutoff frequency is proportional to the SECS of laser crystal. Therefore, it is expected that employing a gain medium with the small SECS would realize low-intensity-noise operation of a laser.

2. Experimental setup

In order to investigate the influence of SECS on the intensity noise of single-frequency laser and further obtain a low-intensity-noise 1080 nm laser, a bow-tie unidirectional ring laser resonator is designed and built as shown in figure 2. The input coupler M_1 is a plane mirror coated with high transmission (HT) film at pump laser ($T > 95\%$) and high reflection (HR) film at 1080 nm ($R_{1080} > 99.5\%$). M_2 is the output coupler coated with partial transmission film of $T = 4\%$ at 1080 nm. Mirrors M_3, M_4 are two plane-concave mirrors with curvature radii of $R = -50$ mm. M_3 and M_4 are coated with HR film at 1080 nm ($R_{1080} > 99.5\%$). Beyond that, M_4 is also coated with HT film at 540 nm ($T_{540} > 95\%$). As a result, the generated 1080 nm and the doubled frequency 540 nm lasers leak from M_2 and M_4, respectively. To realize a good mode-matching with the stable resonator mode, the pump laser is

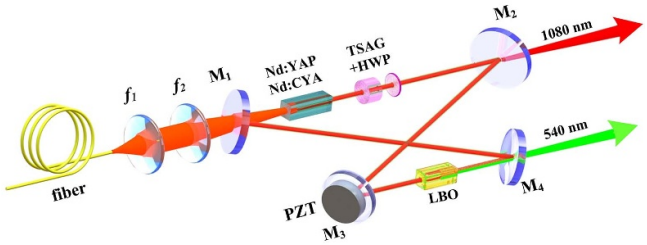


Figure 2. Schematic diagram of the LD-pumped CW SLM dual-wavelength 1080 and 540 nm laser.

Table 2. Physical characteristics of Nd:YAP and Nd:CYA crystals.

Parameters	Nd:YAP [30, 31]	Nd:CYA [27, 32–35]
Thermal conductivity		3.7(‖ a)
(W (m·K)$^{-1}$)	11	3.3(‖ c)
Thermo-optical coefficient	9.7 (‖ a)	−7.8 (‖ a)
(10^{-6} K^{-1})	14.5 (‖ c)	−8.7 (‖ c)

shaped and further focused to the gain medium by employing a telescope system consisting of f_1 ($f_1 = 30$ mm) and f_2 ($f_2 = 50$ mm). The combination of a terbium scandium aluminum garnet (TSAG) crystal and a half-wave plate (HWP) act as optical diode is inserted into the resonator to eliminate the spatial hole burning effect and ensure the unidirectional operation of the laser [20, 21]. The intracavity frequency-doubling crystal, type-I non-critical phase-matching lithium triborate (LBO) crystal with the dimensions of $3 \times 3 \times 15$ mm^3, is placed at the high focus between the mirrors M_3 and M_4. The phase-matching temperature of the LBO crystal is set at 136.9 °C. With the introduced sufficient nonlinear loss, the laser could work with stable single-longitudinal-mode (SLM) operation [22–24]. In the experiment, to reduce the influence of the environment vibrations including temperature variation and air fluctuations, the laser system is fixed on an optical platform, the whole elements of the laser resonator are integrated in a sealed and temperature stabilized aluminum cavity.

As comparison, both laser gain media of Nd:YAP and Nd:$CaYAlO_4$ (Nd:CYA) crystals are employed in the experiment to emit fundamental wave 1080 nm laser. Detailed information about the spectroscopic properties of the two laser media above could be found in references [25–29]. In order to eliminate the influence of other factors, the resonator parameters including the resonator length of 283.84 mm and transmission of output coupler of $T_{1080} = 4\%$ are the same. The thermal conductivity and thermo-optical coefficient of the Nd:YAP crystal are listed in table 2. In order to match the absorption band of Nd:YAP crystal, a fibre-coupled LD (Dilas, Co., Ltd) with the central wavelength of 803 nm acts as the pump source. The core diameter and numerical aperture (NA) of the fibre are 400 m and 0.22, respectively. The dimensions and Nd-doping concentration of the b-cut cylindrical Nd:YAP crystal are diameter 3×15 mm^3 and 0.4 at.%, respectively. Both ends of the crystal are coated with antireflection (AR) films at 803 nm and

1080 nm. In the experiment, the Nd:YAP crystal is wrapped with indium foil in a copper oven controlled by a temperature controller with the precision of 0.01 °C. The crystallography *c*-axis of the Nd:YAP crystal is exactly parallel to the sagittal plane of the resonator to generate the 1080 nm laser with the vertical polarization. And the designed wedge angle of 1.5° at the rear end face acts as a polarizing beam splitter to further improve the polarization degree of the emitted 1080 nm laser.

Different from the Nd:YAP crystal, Nd:CYA is a kind of crystal with negative thermo-optical coefficients and small thermal coefficient of the optical path (1.2×10^{-6} K^{-1}) [27, 32–35]. The corresponding thermo-optical coefficients and thermal conductivities are listed in table 2. It is lucky that the wavelength of the pump LD is easy to be matched because the absorption peak and inhomogeneous absorption spectrum are around 807 nm ($^4I_{9/2} \rightarrow {}^4F_{5/2}+{}^2F_{9/2}$) and as large as 5 nm (full width at half maximum), respectively [29]. Therefore, a fibre-coupled LD (Dilas, Co., Ltd) with the central wavelength of 808 nm is adopted to pump the Nd:CYA crystal. The dimensions of the adopted α-cut Nd:CYA crystal are of $3 \times 3 \times 6$ mm^3. Both ends are coated with AR films at the wavelength of pump laser and oscillating laser. Inversely, in order to adapt the phase-matching condition of the LBO crystal and further improve the optical conversion efficiency as well as obtain the 1080 nm laser with high polarization as much as possible, the crystallography *c*-axis of the crystal is exactly adjusted to be parallel with the resonator's tangential plane in the experiment.

3. Experimental results

In the experiment, the Nd:YAP crystal is firstly used as the gain medium. The output power curve of the 1080 nm laser, illustrated in figure 3, shows that the maximum output powers of emitted 1080 and 540 nm lasers reach up to 1.97 W and 182.75 mW (PM30, Coherent Co., Ltd), respectively, when the pump power is 15.16 W. In this case, the best mode-matching is achieved [36, 37], and the measured threshold pump power and slope efficiency are 9.18 W and 32.95%, respectively. It is clear that the nonlinear output trend is observed, which results from the positive thermal lens effect and the nonlinear loss introduced by the LBO crystal. When the output power is up to 1.96 W, the long-term power stability of Nd:YAP laser is tested by a power meter (PM30, Coherent Co., Ltd) with 3-digit accuracy. The acquisition time and sample rate are set as 6 hours and one per second, respectively. The obtained power trend is depicted in figure 4(a). It is clear that the measured peak-to-peak power fluctuation during 6 h is less than $\pm1.09\%$. Figure 4(b) and its inset reveal the representative recorded caustic curve and the corresponding spatial beam profile of the Nd:YAP laser, respectively (M2SET-BP209IR/M, Thorlabs Co., Ltd). In order to improve the measurement precision, many measurements are implemented in the experiment. The attained beam qualities are $M_x^2 = 1.16\pm0.01$ and $M_y^2 = 1.17\pm0.01$, respectively. Figure 4(c) depicts the longitudinal-mode structure of the Nd:YAP laser, which is

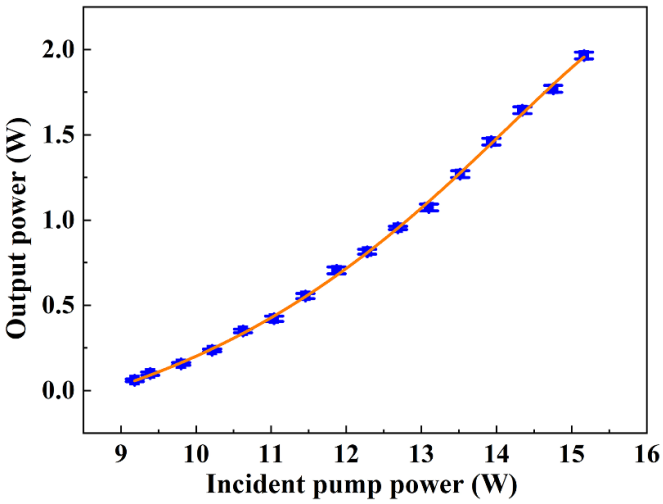


Figure 3. Output power of Nd:YAP laser as a function of the incident pump power (The blue dots are the measured powers at 1080 nm, the orange solid line is the corresponding fitting curve).

monitored by a scanned temperature-controlled Fabry–Perot cavity (F-P-100, Yuguang Co., Ltd) with the free spectral range (FSR) and finesse of 750 MHz and 120, respectively. It reveals that the laser is running in stable SLM operation, which is ascribed to the enough nonlinear loss introduced by the frequency-doubled crystal LBO to suppress the multi-mode oscillation and mode hopping. At the same time, the 1080 nm laser linewidth is measured by employing a delayed self-heterodyne interferometer [7, 38, 39] with a fast detector (PDA8GS, S/N29637, Thorlabs) and a path length imbalance of 25 km between the long and short branches of the interferometer. To prevent the influence from ambient vibration and $1/f$ noise in the detection circuit, the laser frequency of the short branch is shifted 150 MHz by an acousto-optical modulator (AOM) (T-M150-0.4C2G-3-F2P, Gooch&Housego) used as the frequency shifter. In the measurement process, the resolution bandwidth and video bandwidth are 200 and 1 Hz, respectively, and the integration time is set as 10 s. The final measured Nd:YAP laser linewidth data with the frequency relative to 150 MHz and the Gaussian line-shape function fitting result are depicted in figure 4(d), wherein the linewidth of the Nd:YAP laser is 120 ± 0.2 kHz.

However, when the Nd:CYA crystal is inserted into the resonator to become the gain medium, the nonlinear output trend different from the Nd:YAP laser is observed and illustrated in figure 5, which is attributed to the weak thermal lens effect of Nd:CYA crystal and the nonlinear loss caused by LBO. When the pump power is 13.78 W, the maximum output power of emitted 1080 nm and 540 nm lasers are 1.12 W and 53.50 mW, respectively. The obtained threshold pump power and optical conversion efficiency of 1080 nm laser are 10.53 W and 34.46%, respectively. The experimental results demonstrate that the optical conversion efficiency can be increased by optimizing the crystal parameters, although the SECS of Nd:CYA is smaller than that of Nd:YAP. When the output power of the Nd:CYA laser is 1.04 W, the peak-to-peak power

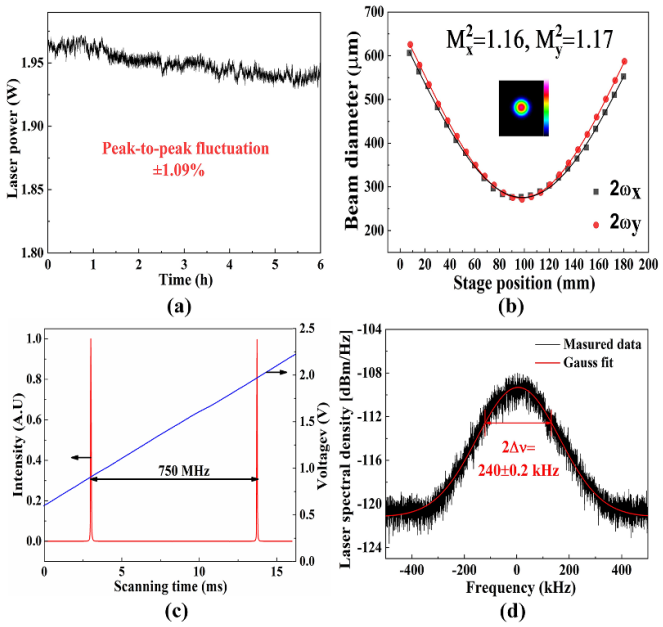


Figure 4. Measured results of the Nd:YAP laser. (a) Power stability in 6 h, (b) beam qualities, (c) longitudinal-mode structure, (d) laser linewidth.

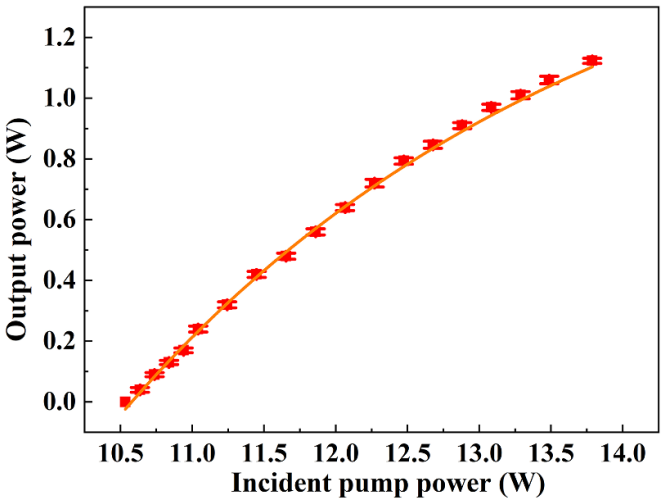


Figure 5. Output power of Nd:CYA laser at 1080 nm as a function of the incident pump power (The red dots are the measured powers at 1080 nm, the orange solid line is the corresponding fitting curve).

fluctuation is tested with the same acquisition time and sample rate of Nd:YAP laser. The tested power fluctuation in 6 h is better than ±0.88% as depicted in the inset of figure 6(a). The beam quality of the Nd:CYA laser is measured by the M^2 meter, and the attained beam qualities of the Nd:CYA laser are $M_x^2 = 1.12 \pm 0.01$ and $M_y^2 = 1.09 \pm 0.01$, respectively. The representative recorded caustic curve and the corresponding spatial beam profile are depicted in the inset of figure 6(b). The longitudinal-mode structure of the laser is also monitored by the same scanned Fabry–Perot cavity, and the monitored transmission curve is shown in figure 6(c). It could be seen that the Nd:CYA laser is also operating in a stable SLM. The measured

Figure 6. Measured results of the Nd:CYA laser. (a) Power stability in 6 h, (b) beam qualities, (c) longitudinal-mode structure, (d) laser linewidth.

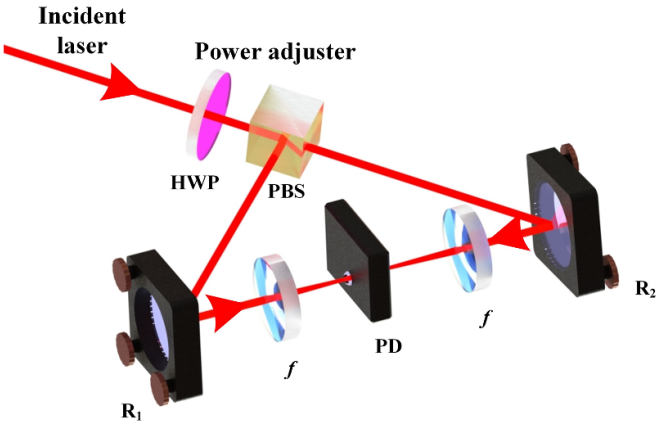


Figure 7. Relative intensity noise measurement platform of 1080 nm lasers.

linewidth of the Nd:CYA laser is 156 ± 0.2 kHz according to the Gaussian line-shape function fitting results as depicted in figure 6(d) with the frequency relative to 150 MHz. The small difference with the Nd:YAP laser comes from the inherent properties of both crystals.

At last, the intensity noise characteristics of both designed Nd:YAP and Nd:CYA lasers are compared and investigated. To this end, a relative intensity noise (RIN) measurement platform including a power adjuster, a homemade self-homodyne detector (Yuguang Co., Ltd), two reflectors (R_1 and R_2) and two identical focusing lenses (f) is set up as shown in figure 7. The self-homodyne detector is made of a pair of identical photodiodes (PD, ETX 500, JDSU Corporation) and the common mode rejection ratio is as high as 60 dB. The power of the incident 1080 nm laser is 2 mW, which is average divided into two parts of 1 mW. One is reflected by PBS and R_1 and

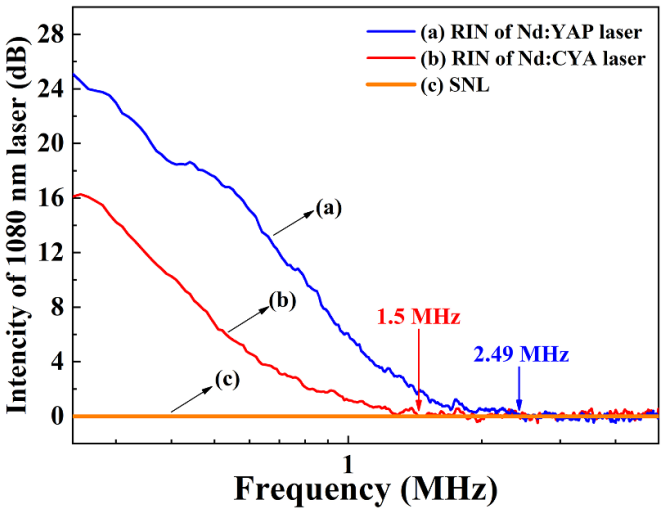


Figure 8. Normalized intensity noise of the 1080 nm lasers.

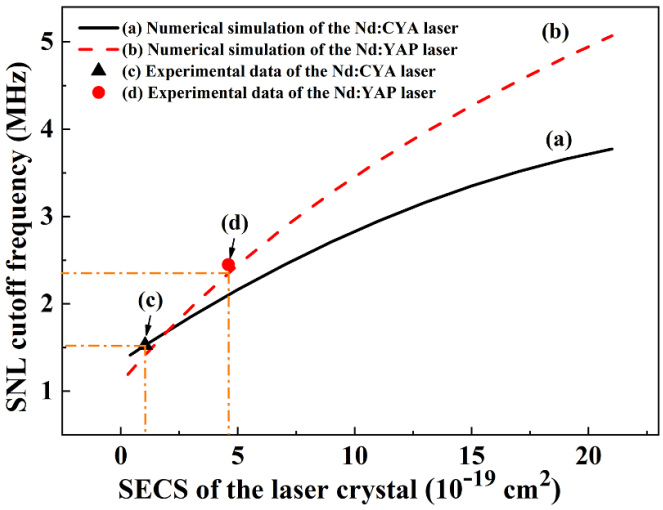


Figure 9. Theoretical prediction of the SNL cutoff frequency versus the SECS of laser crystal.

focused into the PD by lens f. The other leaked from the PBS is reflected by R_2 and focused on PD by another lens f. The detected signal is recorded by a spectrum analyzer (N9010A ATO-22702, Aligent Corporation) [38, 40]. According to the relationship of $V_{obs} = V_2 - (V_1 - 3dB)$, the RIN spectrum of the measured 1080 nm laser could be extracted, where V_1 represents the subtracted signal spectrum of these two PDs, V_2 represents either PD's signal spectrum illuminated with 1 mW. In the measurement process, the resolution bandwidth and video bandwidth are 30 kHz and 30 Hz, respectively. Considering the balanced homodyne detector operates with low-noise, high-gain and high common mode rejection ratio in a large frequency range from 200 kHz to 5 MHz, meanwhile, the cutoff frequencies of common solid-state single-frequency CW lasers reach SNL below 5 MHz, we set the detection frequency ranges from 200 kHz to 5 MHz to display the intensity noise of 1080 nm lasers in details. To address the problem of the output power difference, the intensity noise of the Nd:YAP laser is normalized to that of the Nd:CYA laser as shown in figure 8, so the intensity noise versus SECS of the laser crystal is comparable. The blue solid (a) and red dash (b) lines represent the intensity noise of the Nd:YAP and Nd:CYA lasers, respectively, and (c) represents the SNL. It could be obviously seen that the intensity noise of the Nd:YAP laser reaches SNL at the frequency of 2.49 MHz. However, the intensity noise of the Nd:CYA laser already reaches SNL at 1.5 MHz. In other words, the intensity noise of the laser is effectively suppressed by utilizing the Nd:CYA crystal to replace the Nd:YAP crystal as the gain medium. Moreover, the RRO peaks of the lasers are effectively suppressed, which are attributed to the nonlinear loss introduced by the second-harmonic generation [38].

Based on the laser parameters and the previous theory, the dependence of the SNL cutoff frequency on SECS of the gain medium is further quantitatively simulated and depicted in figure 9. For Nd:YAP laser, crystal length and Nd-doping concentration of Nd:YAP crystal are 15 mm and 0.4%, respectively. Meanwhile, the wavelength of the pump source and pump power are 803 nm and 15.16 W, respectively. In this case, the measured intensity noise of the pump field is 38.32 dB. According to the theoretical simulation and experimental results of intensity-noise spectrum for the free-running laser with varying levels of pump noise in [41, 42], there was hardly any change in the intensity-noise spectrum near and above the RRO frequency as increasing the pump noise. Whereas, it was evident that the pump noise had a great influence on the intensity-noise spectrum below the RRO frequency. So the pump noise has not too much association with the SNL cutoff frequency. For Nd:CYA laser, the length and Nd-doping concentration of the laser gain crystal are 6 mm and 1%, respectively. The wavelength of the pump source and pump power are 808 nm and 13.78 W, respectively, wherein the measured pump intensity noise is 43.04 dB above SNL. In figure 9, the black solid curve (a) and red dash curve (b) represent numerical simulations of the dependence of SNL cutoff frequency on SECS of Nd:YAP and Nd:CYA laser mediums, respectively. (c) and (d) represent the theoretical predictions for Nd:CYA laser with $\sigma_{sNd:CYA} = 1.04 \times 10^{-19}$ cm^2 [33] and Nd:YAP laser with $\sigma_{sNd:YAP} = 4.6 \times 10^{-19}$ cm^2 [30], respectively. It is worth noting that, benefited from the disordered structure [25], the SECS of Nd:CYA crystal is only about a quarter of that of Nd:YAP crystal at 1080 nm. As depicted in figure 9, it is obvious that SNL cutoff frequency shifts to low frequency with the decrease of SECS of gain medium. Especially, it is depicted that the frequencies of the Nd:YAP and Nd:CYA lasers intensity noise reach SNL at 2.37 MHz and 1.53 MHz, respectively. The numerical simulations have a good agreement with the experimentally measured results. Both that the intensity noise of the laser can be effectively suppressed by adopting a laser crystal with small SECS as the gain medium. The laser characteristics of the experimental results and the theoretical prediction reveal intensity noise and output power would be better if we further choose a more suitable crystal and optimize the crystal length as well as doping concentration.

4. Conclusion

We develop an effective approach to realize a single-frequency laser with low intensity noise by employing a crystal with the small SECS to decrease the SER G. Through experimentally replacing the adopted gain medium of Nd:YAP crystal by Nd:CYA crystal, whose SECS is only about a quarter of that of Nd:YAP crystal at 1080 nm, the cutoff frequency of the measured intensity noise obviously reduces from 2.49 MHz to 1.5 MHz, which fit well with the theoretical predictions. On this basis, we successfully realize a low-intensity-noise single-frequency CW 1080 nm laser with high stabilities by utilizing Nd:CYA as the gain medium for the first time. The maximal output power of SLM CW Nd:CYA laser reaches up to 1.12 W. The beam qualities of 1080 nm laser are better than $M_x^2 = 1.12\pm0.01$ and $M_y^2 = 1.09\pm0.01$. Our work will provide a helpful reference for the development of SLM CW 1080 nm lasers with high power and low intensity noise. And the obtained low-intensity-noise single-frequency CW 1080 nm laser as a promising light source will play important role in the generation of high squeezed degree and correlations of the squeezed state light and entangled state.

Acknowledgments

This work was supported by the National Natural Science Foundation of China (61975100, 62027821, 62105192), the Program for the Innovative Talents of High Education Institutions of Shanxi and the Fund for Shanxi '1331 Project' Key Subjects Construction. The authors declare no conflicts of interest.

References

[1] Kuwamoto T, Honda K, Takahashi Y and Yabuzaki T 1999 *Phys. Rev.* A **60** R745
[2] Wineland D J and Itano W M 1979 *Phys. Rev.* A **20** 1521
[3] Chen M, Menicucci N C and Pfister O 2014 *Phys. Rev. Lett.* **112** 120505
[4] Abbott B P *et al* 2016 *Phys. Rev. Lett.* **116** 061102
[5] Wang Y, Shen H, Jin X L, Su X L, Xie C D and Peng K C 2010 *Opt. Express* **18** 6149
[6] Su X L, Hao S H, Deng X W, Ma L Y, Wang M H, Jia X J, Xie C D and Peng K C 2013 *Nat. Commun.* **4** 2828
[7] Guo Y R, Lu H D, Peng W N, Su J and Peng K C 2019 *Opt. Lett.* **44** 6033
[8] Lam P K, Ralph T C, Huntington E H and Bachor H A 1997 *Phys. Rev. Lett.* **79** 1471
[9] Zhang J, Ma H L, Xie C D and Peng K C 2003 *Appl. Opt.* **42** 1068
[10] Winkelmann L *et al* 2011 *Appl. Phys.* B **102** 529
[11] Willke B, Uehara N, Gustafson E K, Byer R L and King P J 1998 *Opt. Lett.* **23** 1704
[12] Chen Y L, Zhang J, Li Y M, Zhang K S, Xie C D and Peng K C 2001 *Chin. J. Lasers* **28** 197
[13] Yu J, Qin Y, Yan Z H, Lu H D and Jia X J 2019 *Opt. Express* **27** 3247
[14] Guo Y R, Peng W N, Su J, Lu H D and Peng K C 2020 *Opt. Express* **28** 5866
[15] Lu H D, Guo Y R and Peng K C 2015 *Opt. Lett.* **40** 5196
[16] Harb C C, Ralph T C, Huntington E H, McClelland D E and Bachor H A 1997 *J. Opt. Soc. Am.* B **14** 2936
[17] Kajima M, Kusumi N, Moriwaki S and Mio N 1999 *Phys. Lett.* A **263** 251
[18] Ludlow A D, Huang X, Notcutt M, Zanon-Willette T, Foreman S M, Boyd M M, Blatt S and Ye J 2007 *Opt. Lett.* **32** 641
[19] Bartolo R E, Tveten A B and Dandridge A 2012 *IEEE J. Quantum Electron.* **48** 720
[20] Jin P X, Lu H D, Yin Q W, Su J and Peng K C 2018 *IEEE J. Sel. Top. Quantum electron.* **24** 1600505
[21] Zhao J Q, Wang Y Z, Yao B Q and Ju Y L 2010 *Laser Phys. Lett.* **7** 135
[22] Martin K I, Clarkson W A and Hanna D C 1997 *Opt. Lett.* **22** 375
[23] Lu H D, Sun X J, Wang M H, Su J and Peng K C 2014 *Opt. Express* **22** 24551
[24] Eismann U, Bergschneider A, Sievers F, Kretzschmar N, Salomon C and Chevy F 2013 *Opt. Express* **21** 9091
[25] Schearer L and Leduc M 1986 *IEEE J Quantum Elect.* **22** 756
[26] Kaminski A A, Sarkisov S E, Mochalov I V, Aminov L K and Ivanov A O 1979 *Phys. Status Solidi* **51** 509
[27] Horacia R V and Leonard M T 1990 *Appl. Phys. Lett.* A **56** 608
[28] Yamaji A, Suzuki A, Shoji Y, Kurosawa S, Pejchal J, Kamada K, Yokota Y and Yoshikawa A 2014 *J. Cryst. Growth* **393** 138
[29] Li D Z, Xu X D, Meng J Q, Zhou D H, Wu F and Xu J 2010 *Opt. Express* **18** 18649
[30] Sulc J, Jelinkova H, Jabczyski J K, Zendzian W, Kwiatkowski J, Nejezchleb K and Skoda V 2005 *Proc. SPIE - Int. Soc. Opt. Eng.* **5707** 325
[31] Lu Q, Kugler N, Weber H, Dong S, Moller N and Wittrock U 1996 *Opt. Quantum Electron.* **28** 57
[32] Zhou D H, Xu X D, Chen X Y, Zhu H M, Li D Z, Di J Q, Xia C T, Wu F and Xu J 2012 *Phys. Status Solidi* a **209** 730
[33] Li D Z *et al* 2011 *J. Opt. Soc. Am.* B **28** 1650
[34] Lv S Z, Zhu Z J, Wang Y, You Z Y, Li Z Y and Tu C Y 2013 *J. Lumin.* **144** 117
[35] Yang H Q, Jin P X, Su J, Xu X D, Xu J and Lu H D 2022 *Chin. Opt. Lett.* **20** 031403
[36] Chen Y F, Kao C F, Huang T M, Wang C L and Wang S C 1997 *IEEE J. Sel. Top Quantum* **3** 29
[37] Xu M Z, Zhang T, Guo Y R, Peng W N and Lu H D 2019 *J. Quantum Opt.* **25** 221
[38] Guo Y R, Lu H D, Xu M Z, Su J and Peng K C 2018 *Opt. Express* **26** 21108
[39] Guo Y R, Xu M Z, Peng W N, Su J, Lu H D and Peng K C 2018 *Opt. Lett.* **43** 6017
[40] Jin X L, Su J, Zheng Y H, Chen C Y, Wang W Z and Peng K C 2015 *Opt. Express* **23** 23859
[41] Harb C C, Ralph T C, Huntington E H, Freitag I, McClelland D E and Bachor H A 1996 *Phys. Rev.* A **54** 4370
[42] Ralph T C, Harb C C and Ba Chor H A 1996 *Phys. Rev.* A **54** 4359